Theoretical Analyses on Short-Term Stability of Semiconductor Fiber Ring Lasers

Qianfan Xu and Minyu Yao

***Abstract*—Detailed analyses of the short-term stability of the semiconductor fiber ring laser (SFRL) are presented. Analysis with rate equations shows that the relaxation oscillation effect does not exist in the SFRL. With a frequency-domain model, the mode competition in the SFRL is shown to be suppressed by the gain saturation effect of the semiconductor optical amplifier. Thus the observed good short-term stability of SFRL is theoretically explained. The analyses are verified in experiments.**

***Index Terms*—Mode competition, relaxation oscillation, semiconductor fiber ring laser, short-term stability.**

I. Introduction

A SEMICONDUCTOR fiber ring laser (SFRL), a fiber ring laser with a semiconductor optical amplifier (SOA) as the gain medium, has many potential applications in optical fiber communication systems. In reported experiments, SFRLs have been successfully applied in tunable lasers [1], [2], multiwavelength optical sources [3]–[5], short-pulse generation [4]–[6], and all-optical clock recovery [7], [8]. Compared with the widely-used erbium-doped fiber laser (EDFL), the SFRL possesses the following advantages: it has good short-term stability, it can generate multiwavelength oscillation at room temperature, and it can be directly mode locked at high bit-rate by optical injection. These advantages enable the SFRL to be used in all-optical clock recovery and multiwavelength continuous-wave (CW) or mode-locked laser sources with very simple configurations.

The high short-term stability of the SFRL has been observed in experiments, and has been attributed, without detailed analysis or calculation, to the absence of relaxation oscillation in the ring [6]. However, to the best of our knowledge, no theoretical analysis on this topic has been presented. In this paper, we will give a detailed and quantitative analysis of the short-term stability of the SFRL.

In fiber ring lasers, short-term stability is determined by two mechanisms: one is the relaxation oscillation and the other is the mode competition [9]–[11]. Fiber ring lasers have long cavities, usually in the order of 10 m. So the frequency difference between the neighboring oscillation modes usually is several megahertz, which is much smaller than the bandwidth of the gain medium ($\sim$ THz) and the optical filter in the ring ($\sim$ 100 GHz). Thus, the side modes have almost the same small-signal gain as the dominant mode in the cavity, and single mode operation cannot be guaranteed. A very small environmental disturbance will induce coupling between the dominant mode and the side modes, and cause fluctuation of the optical power. When relaxation oscillation exists, optical power fluctuation—generated by the interference between different modes—will persist and in turn induces more mode coupling. This phenomenon can be easily observed in EDFLs, where clean outputs are hardly obtained without special configuration or adjustment. However, a SFRL, with its simplest configuration, gives clean CW laser output. As we will indicate in this paper, one reason is that there is no relaxation oscillation in the SFRL; the other is that the mode competition in the SFRL is significantly suppressed by the gain saturation effect of SOA.

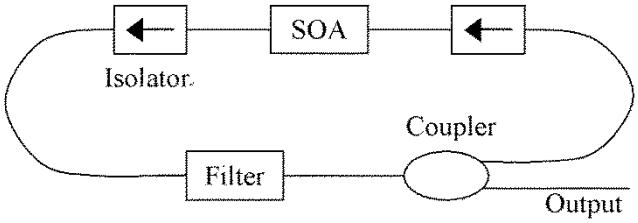

Fig. 1. Basic structure of a CW semiconductor fiber ring laser.

In harmonically mode-locked fiber ring lasers, the long-term stability is also an important issue. The total optical length of the cavity fluctuates with the fluctuation of environmental temperature. When the change of the optical length of the cavity is comparable to c/f, where c is the light velocity and f is the mode-locking frequency, the quality of the output pulses will be degraded. Since the total length of the SFRL can be as short as a few meters, the mode-locked SFRL can potentially achieve high long-term stability even when no active cavity length control is present. However, this paper focuses on short-term stability only.

This paper is organized as follows. In Section II, the relaxation oscillation frequency of the SFRL is calculated with rate equations and is shown to be a pure imaginary, which means relaxation oscillation does not exist in the SFRL. In Section III, theoretical understanding and calculation of the nonlinear suppression of mode competition in the SFRL are presented with a small-signal frequency-domain model of SOA. The calculation result is verified experimentally in Section IV.

II. Analysis of Relaxation Oscillation

Fig. 1 is the basic structure of a CW SFRL. The SFRL can be harmonically mode locked by inserting an intensity modulator in the ring, or by injection of external optical pulses.

Manuscript received March 3, 2003; revised June 24, 2003. This work was supported by the Natural Science Foundation Committee of China (NSFC 60077001) and by Tsinghua University Research Foundation.

The authors are with the Department of Electronic Engineering, Tsinghua University, Beijing 100084, China (e-mail: qx23@cornell.edu).

Digital Object Identifier 10.1109/JQE.2003.817668

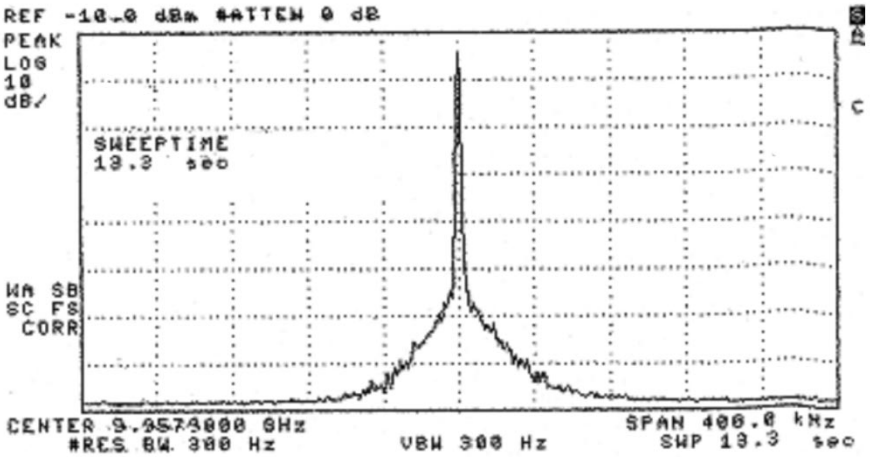

Fig. 2. Output power spectrum of the SFRL mode-locked at 9.9578 GHz. The frequency span is 400 kHz, centered at 9.9578 GHz. The vertical scale is 10 dB per division.

Suppose n is the total number of carriers and N is the total number of photons in the SFRL. Then the rate equations of the SFRL are

$$\frac{dn}{dt} = \frac{I}{q} - \frac{n}{\tau_c} - g(n)\cdot N \tag{1}$$

$$\frac{dN}{dt} = g(n)\cdot N - \frac{N}{\tau_p} + A(n) \tag{2}$$

where I is the bias current of the SOA, q is the electron charge, τ_c is the carrier lifetime, τ_p is the photon lifetime, g is the rate of stimulated emission per photon, and A is the rate of spontaneous emission within the bandwidth of interest.

When the SFRL is working around its steady state, g and A are linearly dependent on the number of carriers. We assume that $n = n_0 + \Delta n$, $N = N_0 + \Delta N$, $g(n) = g_0 + a\cdot\Delta n$, and $A(n) = A_0 + \beta\cdot\Delta n$, where Δn and ΔN are small disturbances. By neglecting the higher order disturbance, we get the following small-signal rate equations:

$$\frac{d\Delta n}{dt} = -\frac{\Delta n}{\tau_c} - (a\Delta n N_0 + g_0\cdot\Delta N) \tag{3}$$

$$\frac{d\Delta N}{dt} = a\Delta n\cdot N_0 + g_0\cdot\Delta N + \beta\Delta n - \frac{\Delta N}{\tau_p}. \tag{4}$$

From (3) and (4), we get a second-order differential equation of ΔN

$$\frac{d^2\Delta N}{dt^2} + \left(\frac{1}{\tau_c} + aN_0 + \frac{1}{\tau_p} - g_0\right)\cdot\frac{d\Delta N}{dt} + \left[\frac{1}{\tau_c}\left(\frac{1}{\tau_p} - g_0\right) + \frac{aN_0}{\tau_p} + g_0\beta\right]\cdot\Delta N = 0. \tag{5}$$

The form of (5) is the same as the equation for damped oscillations. Their solution should be of the form of e^{kt}, where the imaginary part of k corresponds to the relaxation oscillation frequency.

For a typical SFRL with 40-m fiber loop and 6-dB loop loss, the photon lifetime τ_p is about 100 ns. On the other hand, typical SOA has a carrier lifetime of about 300 ps, which is much smaller than τ_p. Normally, the SOA is biased well above the threshold current, so the contribution of the in-band spontaneous emission is much smaller that the contribution of stimulated emission

$$\begin{cases} \frac{1}{\tau_c} \gg \frac{1}{\tau_p} \\ \frac{1}{\tau_p} \approx g_0 \gg \frac{1}{\tau_p} - g_0 > 0 \end{cases}. \tag{6}$$

Thus, the approximate values of two solutions of k are

$$k_1 \approx -\frac{1}{\tau_p}\cdot\left(1 - \frac{g_0\tau_p}{1 + aN_0\tau_c}\right) < 0 \tag{7}$$

$$k_2 \approx -\frac{1}{\tau_c}\cdot(1 + aN_0\tau_c) < 0. \tag{8}$$

Since k_1 and k_2 are both negative real numbers, there is no relaxation oscillation, and the solution of differential (5) $\Delta N = C_1\cdot e^{k_1 t} + C_2\cdot e^{k_2 t}$ is a decay function with time. This solution implies that if environmental disturbance induces a small derivation in optical power or gain, the derivation will decrease monotonously with time, and the SFRL will get back to steady state quickly.

In many practical applications, SFRLs are harmonically mode locked at high frequency (> 10 GHz). In these applications, since the pulse period is smaller than the characteristic time of the rate equations τ_c and τ_p, the former calculation is also valid by taking ΔN and Δn as the average over one period.

In the power spectrum of an EDFL, we can easily see the spectral component corresponding to the relaxation oscillation [11]. However, we cannot observe the relaxation oscillation spectral component in Fig. 2, which is the power spectrum of the output of a SFRL mode-locked at 10 GHz. This verified the conclusion that no relaxation oscillation exists in the SFRL. Note that the approximately triangular pedestal in the spectrum is induced by the spontaneous emission noise [12].

III. Analysis of Mode Competition

As mentioned in Section I, the extra-dense side modes in fiber ring lasers cannot be effectively suppressed by the optical filter

or gain medium. Usually, many side modes oscillate and compete with the dominant mode. Large environmental disturbance will even cause the dominant mode change from one mode to another constantly. The interference between the side modes and the dominant mode will make the output of fiber ring lasers very noisy. However, if the gain medium in the fiber ring laser is a SOA, the side modes will be suppressed by the gain saturation effect of the SOA, and the output of the laser will be much cleaner. We denote the side-mode suppression effect coming from wavelength dependent gain and loss as linear suppression, and the suppression effect coming from nonlinear effects, like the gain dynamics of SOA, as nonlinear suppression. In this section, we will calculate the magnitude of nonlinear suppression effect in the SFRL.

Suppose one dominant mode and one weak side mode exist in the SFRL. And the small signal gains of the dominant mode and the side mode are equal. The optical field of the dominant mode at the input port of the SOA is $E_0 = E \cdot \cos \omega_0 t$, and that of the side mode is $E_1 = E \cdot \delta_{\rm in} \cdot \cos[(\omega_0 + \Delta\omega)t + \phi]$, with the side mode extinction ratio $\delta_{\rm in} \ll 1$. Then the input optical power of the SOA is

$$\begin{aligned} P_{\rm in} =& \frac{1}{2}(1+\delta_{\rm in}^2)E^2 + \delta_{\rm in}E^2\cos(\Delta\omega\cdot t+\phi) \\ =& \overline{P_{\rm in}} + \Delta P_{\rm in}(t). \end{aligned} \tag{9}$$

The relative variation of the input optical power is defined as

$$R_{\rm in} = \frac{|\Delta P_{\rm in}|_{\max}}{\overline{P_{\rm in}}} = \frac{2\delta_{\rm in}}{1+\delta_{\rm in}^2} \tag{10}$$

so that

$$\Delta P_{\rm in}(t) = R_{\rm in}\overline{P_{\rm in}}\cos(\Delta\omega\cdot t+\phi). \tag{11}$$

We can similarly define the SOA's output side mode extinction ratio $\delta_{\rm out}$ and the relative variation of the SOA's output power $R_{\rm out}$. They will be calculated below with the small-signal dynamic equation of SOA.

The integrated gain of the SOA is [13]

$$h(t) = \int_0^L g(z,t)dz = \overline{h} + \Delta h(t) \tag{12}$$

where the small time-variant term is caused by the variation of input optical power. The time-variant term is determined by the following differential equation [14]:

$$\tau_c \cdot \frac{d\Delta h(t)}{dt} + \left(1 + \frac{\overline{P_{\rm in}}\cdot e^{\overline{h}}}{P_{\rm sat}}\right)\Delta h(t) = -\frac{\Delta P_{\rm in}(t)}{P_{\rm sat}}(e^{\overline{h}}-1) \tag{13}$$

where $P_{\rm sat}$ is the saturate power of SOA [13]. We define a saturation coefficient S to characterize the average depth of saturation: $S = \overline{P_{\rm in}}\cdot e^{\overline{h}}/P_{\rm sat}$, and (13) can be rewritten with (11) as

$$\begin{aligned} \tau_c \cdot \frac{d\Delta h(t)}{dt} &+ (1+S)\Delta h(t) \\ &= -SR_{\rm in}(1-e^{-\overline{h}})\cos(\Delta\omega\cdot t+\phi). \end{aligned} \tag{14}$$

The solution of (13) is

$$\begin{aligned} \Delta h(t) =& \frac{-SR_{\rm in}(1-e^{-\overline{h}})}{(1+S)^2+(\tau_c\Delta\omega)^2} \\ &\cdot[(1+S)\cdot\cos(\Delta\omega\cdot t+\phi) + \tau_c\Delta\omega\cdot\sin(\Delta\omega\cdot t+\phi)]. \end{aligned} \tag{15}$$

The output optical power of the SOA is

$$P_{\rm out} = P_{\rm in}\cdot e^h \approx \overline{P_{\rm in}}\cdot e^{\overline{h}} + \Delta P_{\rm in}(t)\cdot e^{\overline{h}} + \overline{P_{\rm in}}\cdot e^{\overline{h}}\cdot\Delta h(t) \tag{16}$$

where the higher order small signal is neglected. The time-variant term of the output optical power can be obtained with (11), (15), and (16) as

$$\begin{aligned} \Delta P_{\rm out}(t) \approx& \Delta P_{\rm in}(t)\cdot e^{\overline{h}} + \overline{P_{\rm in}}\cdot e^{\overline{h}}\cdot\Delta h(t) \\ =& \overline{P_{\rm in}}R_{\rm in}e^{\overline{h}}\left[\left(1 - \frac{(1+S)S(1-e^{-\overline{h}})}{(1+S)^2+(\tau_c\Delta\omega)^2}\right)\right. \\ &\cdot\cos(\Delta\omega\cdot t+\phi) \\ &\left. - \frac{S(1-e^{-\overline{h}})\cdot\tau_c\Delta\omega}{(1+S)^2+(\tau_c\Delta\omega)^2}\sin(\Delta\omega\cdot t+\phi)\right]. \end{aligned} \tag{17}$$

This result is consistent with the frequency-domain transfer function derived by Sato and Toba [15].

The relative variation of the output optical power of the SOA is

$$R_{\rm out} = \frac{|\Delta P_{\rm out}|_{\max}}{\overline{P_{\rm in}}\cdot e^{\overline{h}}} = \sqrt{1 - \frac{(1+S)^2K(2-K)}{(1+S)^2+(\tau_c\Delta\omega)^2}}\cdot R_{\rm in} \tag{18}$$

where $K = S\left(1-e^{-\overline{h}}\right)/1+S$. Since $0 < K < 1$, it is obvious that $R_{\rm out} < R_{\rm in}$, and because the relative variation R decreases monotonously with the decrease of the side-mode suppression ratio δ when $\delta < 1$, we have $\delta_{\rm out} < \delta_{\rm in}$, which means that the side mode experiences a lower effective gain than the dominant mode, even though their small-signal gains are the same. The lower effective gain will prevent the side mode from oscillating.

The nonlinear suppression effect can be easily understood in the time domain: since the SOA has a higher gain when input optical power is low and vice versa, the power fluctuation of the oscillating laser can be suppressed a bit every time the lightwave passes through the SOA. In the frequency domain, as the above calculation shows, the side modes experience an extra loss from the gain saturation of the SOA and have lower effective gain than the dominant mode. Right after a side mode begins to oscillate due to the environmental disturbance or amplified spontaneous-emission (ASE), when its amplitude is much smaller than the dominant mode, it will be suppressed by gain saturation and will not grow up or compete with the dominant mode.

In the real SFRL, because of the presence of the ASE, many side modes simultaneously exist (have nonzero amplitudes). However, since the amplitudes of the side modes are much smaller than that of the dominant mode, we can neglect the optical power fluctuation caused by the interference between two side modes, and consider the interaction between one side mode and the dominant mode at one time. In other words, the analysis of nonlinear side-mode suppression can be applied to each side mode respectively.

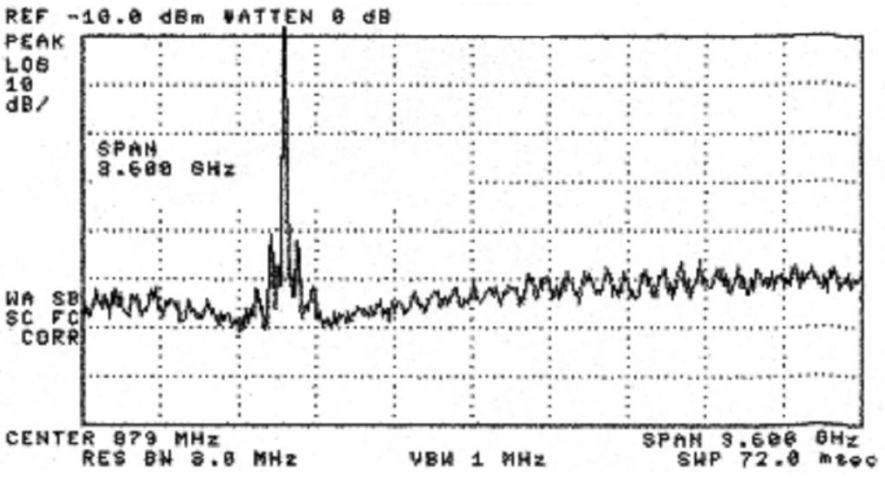

Fig. 3. Output power spectrum of a CW SFRL. The frequency span is from −921 to 2679 MHz. The vertical scale is 10 dB per division.

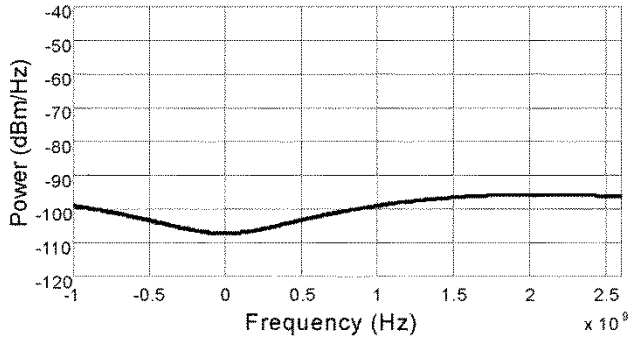

Fig. 4. Calculated envelope of the power spectrum of the side modes in a CW SFRL.

Considering that the side-mode extinction ratios are much smaller than 1, we have

$$\frac{R_{\text{out}}}{R_{\text{in}}} = \frac{\delta_{\text{out}}}{\delta_{\text{in}}} \cdot \frac{1+\delta_{\text{in}}^2}{1+\delta_{\text{out}}^2} \approx \frac{\delta_{\text{out}}}{\delta_{\text{in}}}. \tag{19}$$

Thus the ratio of the effective gain of the side mode to that of the dominant mode is

$$\begin{aligned}\eta(\Delta\omega) =& \frac{G_{\text{side}}}{G_{\text{dorm}}} = \left(\frac{\delta_{\text{out}}}{\delta_{\text{in}}}\right)^2 \approx \left(\frac{R_{\text{out}}}{R_{\text{in}}}\right)^2 \\ =& 1 - \frac{(1+S)^2K(2-K)}{(1+S)^2+(\tau_c\Delta\omega)^2}. \end{aligned}\tag{20}$$

The parameter η will be used to characterize the magnitude of the nonlinear suppression. From (20), we see that η decreases with the decrease of $\Delta\omega$, so the side modes close to the dominant mode in frequency (with small $\Delta\omega$) will be better suppressed than those far from the dominant mode (with large $\Delta\omega$). For the side modes adjacent to the dominant mode, $\tau_c\Delta\omega \ll 1$ and $\eta \approx (1-K)^2$. When $\Delta\omega \to \infty$, $\eta \to 1$, and the suppression effect would be very weak. However, since the side modes far away from the dominant mode in frequency have lower small-signal gain from the SOA and larger loss from the optical filter in the loop, these modes would be suppressed by the linear suppression effect. When $\Delta\omega$ is fixed, larger average input optical power corresponds to higher S and K, and lower η. So side modes will be better suppressed when the SOA is deeper saturated.

In a typical EDFL, the upper level lifetime of Er-doped fiber ($\sim$ ms) is much longer than the period of power fluctuation caused by mode competition. So, similar to the situation when $\tau_c\Delta\omega \gg 1$ in the SFRL, the nonlinear suppression effect in EDFL is very weak even for the side modes adjacent to the dominant mode and cannot suppression mode competition effectively. To get acceptable performance, some additional nonlinear effects, like nonlinear polarization rotation [16] or two-photon absorption [17], can be introduced into the ring. The performance of these nonlinear effects in the EDFL can be analyzed in the frequency domain similarly.

From (17), we see that gain dynamics in the SOA also induce a phase change in optical power fluctuation. It is clear from (9) that the phase of power fluctuation is equal to the phase of the side mode. Therefore, the side modes will get an additional phase change from the gain dynamics when they pass through the SOA. Unfortunately, this small phase change is very hard to detect in experiments.

IV. Experimental Verifications

In this section, we will experimentally illustrate that nonlinear suppression effect does exist and is a main contributor to the short-term stability of the SFRL. As shown in Section III, the side modes close to the dominant mode in frequency are better suppressed by nonlinear suppression effect than those far from the dominant mode. The linear suppression has the opposite frequency dependent property. So, we can prove that nonlinear suppression effect dominates in SFRL, if we see, besides the main peak of the DC component, lower noise level at low frequency, and higher noise level at high frequency in the output power spectrum of the CW SFRL.

First, let us give a quantitative analysis on the power spectrum of the side modes in a CW SFRL. Because of the co-existence of the laser oscillation and the ASE, the balance equation of a side

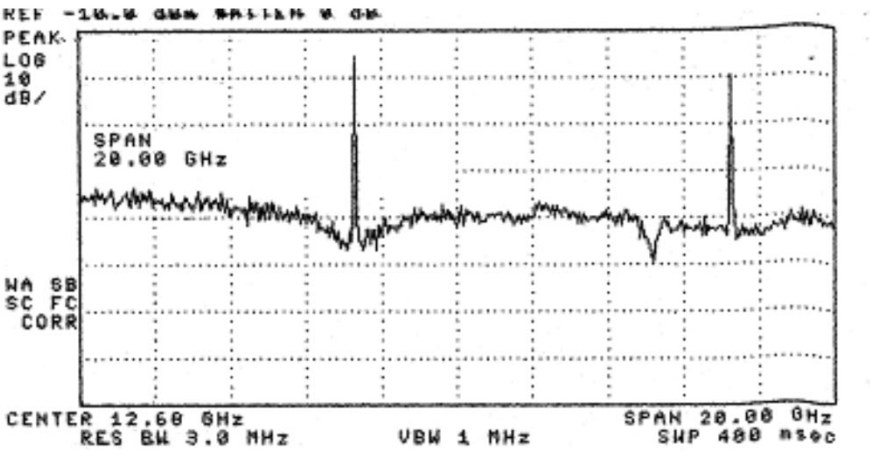

Fig. 5. Output power spectrum of the SFRL mode-locked at 10 GHz. The span of the spectrum is from 2.6 to 22.6 GHz. The vertical scale is 10 dB per division.

mode with the angular frequency $\Delta\omega$ away from the dominant mode is

$$\frac{\eta(\Delta\omega)\cdot G_L}{Lo}P(\Delta\omega)+S=P(\Delta\omega) \tag{21}$$

where $P(\Delta\omega)$ is the power spectrum density of the side mode, G_L is the linear gain of the side mode, which equals $G_{\rm dorm}$ if there is no linear suppression effect, Lo is the loop loss, and S is the power spectrum density of ASE generated by the SOA. Thus

$$P(\Delta\omega)=\frac{S}{1-\eta(\Delta\omega)\cdot\frac{G_L}{Lo}}. \tag{22}$$

In reality, G_L, S, and Lo are all wavelength (frequency) dependent. Within the frequency range we are concerned with, the most significant linear suppression effect comes from the residual reflection at both ends of the SOA, which causes a several tenths of a decibel variation in G_L and S over a frequency span of about 20 GHz. These variations have been taken into account in our calculations.

In the experiment, the output optical signal of a CW SFRL was detected by a p-i-n receiver. The photocurrent was converted into a voltage signal, which was sent to a spectrum analyzer. The time-variant component of the voltage signal is proportional to the optical power variation which, as shown in Section III, is proportional to the field intensity of the side modes. Therefore, the power spectrum of the voltage signal measured by the spectrum analyzer, except for the DC component, should be proportional to the power spectrum of the side modes calculated in (22).

Fig. 3 is the power spectrum obtained in experiment when the SOA is biased at 190 mA, the output optical power is 100 μW, and the wavelength of the output laser is 1553.4 nm. The total length of the ring is about 40 m. From the figure, we can see that the noise level increased about 12 dB from around the DC component to 2 GHz, which shows that the side modes near the dominant mode are suppressed by nonlinear suppression effect. The noise level begins to decrease when the frequency is larger than 2 GHz because the linear suppression effect gradually overwhelms the nonlinear suppression effect as the frequency difference between the side mode and the dominant mode increases. Note that in Fig. 3, the four small peaks immediately adjacent to the main peak are coming from the driving circuit of the SOA. They can be seen at the same frequency even when the SOA is working alone as an ASE source. So, these four peaks have nothing to do with the mode competition or relaxation oscillation.

With (20) and (22), the power spectrum of the side modes is calculated and shown in Fig. 4. The calculated curve fits well with the envelop of the detected power spectrum in Fig. 3. This verified the nonlinear suppression theory developed in Section III. In the calculation, $\tau_c=400$ ps, $S=0.04$, the reflectivity at the end of SOA is taken to be 10^{-4}, and $\overline{h}$ is obtained from equation

$$\log G_0-\overline{h}=S\cdot(1-e^{-\overline{h}}) \tag{23}$$

where G_0, the small-signal gain of SOA, is 23 dB.

The nonlinear suppression theory can also be extended to the harmonically mode-locked SFRL. In a SFRL mode-locked at frequency F, a group of modes with frequency interval F will be coupled together by the modulator and form a supermode. So, the mode competition will be substituted by the supermode competition. The linear gains of the supermodes are almost identical in fiber ring lasers, and thus the supermode competition can only be suppressed by nonlinear effects. The interference between the side supermode and the dominant supermode generates a low frequency power fluctuation, which will be suppressed by gain saturation of SOA. So the side supermode has a lower effective gain than the dominant supermode. The calculation in Section III can be applied by averaging all quantities over a modulation period when $\Delta\omega/2\pi$ is much smaller than F.

Fig. 5 is the measured power spectrum of an SFRL mode-locked at 10 GHz. We can easily see the lower noise level around the 10-GHz spectral component. In the experiment, the modulation frequency was intentionally detuned off the harmonics of the base mode of the loop cavity. When the mode-locked SFRL was not detuned, the amplitude of supermode competition noise was so small that it could hardly be observed by the spectrum

analyzer over a large frequency span. Note that the response of the spectrum analyzer is not uniform over such a large frequency span. For example, the dip around 17 GHz in Fig. 5 is caused by a nonuniform response of the spectrum analyzer.

V. Conclusion

Quantitative analyses show that there is no relaxation oscillation in the SFRL and that mode competition is well suppressed by gain saturation of the SOA, which explains why the SFRL has good short-term stability. The analyses are performed on CW SFRLs. However, they can also be extended to harmonically mode-locked SFRLs. These analyses have been verified by experiments.

References

[1] D. Zhou, P. R. Prucnal, and I. Glesk, "A widely tunable narrow linewidth semiconductor fiber ring laser," *IEEE Photon. Technol. Lett.*, vol. 10, pp. 781–783, 1998.

[2] Z. Hu, F. Li, Z. Pan, and W. Tan, "Wavelength-tunable narrow-linewidth semiconductor fiber-ring laser," *IEEE Photon. Technol. Lett.*, vol. 12, pp. 977–979, 2000.

[3] N. Pleros, C. Bintjas, M. Kalyvas, G. Theophilopoulos, K. Yiannopoulos, S. Sygletos, and H. Avramopoulos, "Multiwavelength and power equalized SOA laser sources," *IEEE Photon. Technol. Lett.*, vol. 14, pp. 693–695, 2002.

[4] B. A. Yu, D. H. Kim, and B. Lee, "Multiwavelength pulse generation in semiconductor-fiber ring laser using a sampled fiber grating," *Opt. Commun.*, vol. 200, pp. 343–347, 2001.

[5] K. Vlachos, K. Zoiros, T. Houbavlis, and J. Avramopoulos, "10×30 GHz pulse train generation from semiconductor amplifier fiber ring laser," *IEEE Photon. Technol. Lett.*, vol. 12, pp. 25–27, 2000.

[6] D. H. Kim, S. H. Kim, Y. M. Jhon, S. Y. Ko, J. C. Jo, and S. S. Choi, "Relaxation-free harmonically mode-locked semiconductor-fiber ring laser," *IEEE Photon. Technol. Lett.*, vol. 11, pp. 521–523, 1999.

[7] D. M. Patrick and R. J. Manning, "20 Gbit/s all-optical clock recovery using semiconductor nonlinearity," *Electron. Lett.*, vol. 30, pp. 151–152, 1994.

[8] K. Vlachos, G. Theophilopoulos, A. Hatziefremidis, and H. Avramopoulos, "30 Gb/s all-optical clock recovery circuit," *IEEE Photon. Technol. Lett.*, vol. 12, pp. 705–707, 1999.

[9] M. Horowitz, C. R. Menyuk, T. F. Carruthers, and I. N. Duling, "Pulse dropout in harmonically mode-locked fiber lasers," *IEEE Photon. Technol. Lett.*, vol. 12, pp. 255–268, 2000.

[10] M. Dong and P. K. Cheo, "Analysis of Er-doped fiber laser stability by suppressing relaxation oscillation," *IEEE Photon. Technol. Lett.*, vol. 8, pp. 1151–1153, 1996.

[11] H. Takara, S. Kawanishi, and M. Saruwatari, "Stabilization of a modelocked Er-doped fiber laser by suppressing the relaxation oscillation frequency component," *Electron. Lett.*, vol. 31, pp. 292–293, 1995.

[12] I. Kim and K. Y. Lau, "Frequency and timing stability of mode-locked semiconductor lasers-passive and active mode locking up to millimeter wave frequencies," *IEEE J. Quantum Electron.*, vol. 29, pp. 1081–1090, 1993.

[13] G. P. Agrawal and N. A. Olsson, "Self-phase modulation and spectral broadening of optical pulse in semiconductor laser amplifiers," *J. Lightwave Technol.*, vol. 25, pp. 2297–2306, 1989.

[14] Q. Xu, M. Yao, M. Chen, and J. Zhang, "Analytical calculation based on probability model for the pattern effect of SOA as in-line amplifier for WDM system," *Opt. Commun.*, vol. 195, pp. 159–166, 2001.

[15] K. Sato and H. Toba, "Reduction of mode partition noise by using semiconductor optical amplifiers," *IEEE J. Select. Topics Quantum Electron.*, vol. 7, pp. 328–333, 2001.

[16] Y. Li, C. Lou, J. Wu, B. Wu, and Y. Gao, "Novel method to simultaneously compress pulses and suppress supermode noise in actively mode-locked fiber ring laser," *IEEE Photon. Technol. Lett.*, vol. 10, pp. 1250–1252, 1998.

[17] E. R. Thoen, M. E. Grein, E. M. Koontz, E. P. Ippen, H. A. Haus, and L. A. Kolodziejski, "Stabilization of an active harmonically mode-locked fiber laser using two-photon absorption," *Opt. Lett.*, vol. 25, pp. 948–950, 2000.

Qianfan Xu received the B.S. degree in 1999 and the M.S. degree in 2002, both in electronic engineering, from Tsinghua University, Beijing, China. In 2002, he spent one year as a graduate student with Purdue University, West Lafayette, IN, majoring in signal processing and communications. He is currently working toward the Ph.D. degree in the School of Electrical and Computer Engineering, Cornell University, Ithaca, NY, conducting research with the nanophotonics group.

His previous research has mostly involved application of the semiconductor optical amplifier in optical fiber communications.

Minyu Yao was born in Shanghai, China, in 1946. She graduated from Tsinghua University, Beijing, China, in 1970.

She is currently a Professor in the Electronic Engineering Department, Tsinghua University. She was a Visiting Associate with California Institute of Technology, Pasadena, from 1994 to 1996. Her research interests include mode-locked fiber ring lasers, various photonic switching, and all-optical signal processing based on the nonlinearities in SOAs and fiber.